Behavior Oriented Data Resource Management in Medical Sensing Systems [1]

HYDUKE NOSHADI, University of California at Los Angeles & Google Inc.
FOAD DABIRI, University of California at Los Angeles & Google In.
SARO MEGUERDICHIAN, University of California at Los Angeles
MIODRAG POTKONJAK, University of California at Los Angeles
MAJID SARRAFZADEH, University of California at Los Angeles

Wearable sensing systems have recently enabled a variety of medical monitoring and diagnostic applications in Wireless Health. The need for multiple sensors and constant monitoring leads these systems to be power hungry and expensive, with short operating lifetimes. We introduce a novel methodology that takes advantage of contextual and semantic properties in human behavior to enable efficient design and optimization of such systems from the data and information point of view. This, in turn, directly influences the wireless communication and local processing power consumption. We exploit intrinsic space and temporal correlations between sensor data while considering both user and system contextual behavior. Our goal is to select a small subset of sensors that accurately capture and/or predict all possible signals of a fully instrumented wearable sensing system. Our approach leverages novel modeling, partitioning, and behavioral optimization, which consists of signal characterization, segmentation and time shifting, mutual signal prediction, and a simultaneous minimization composed of subset sensor selection and opportunistic sampling. We demonstrate the effectiveness of the technique on an insole instrumented with 99 pressure sensors placed in each shoe, which cover the bottom of the entire foot, resulting in energy reduction of 72% to 97% for error rates of 5% to 17.5%.

Categories and Subject Descriptors: C.3 [**Special-Purpose and Application-Based Systems**]: Real-time and embedded systems; B.8.2 [**Performance and Reliability**]: Performance Analysis and Design Aids; J.3 [**Life and Medical Sciences**]: Medical information systems

General Terms: Design, Algorithm, Performance

Additional Key Words and Phrases: Wearable Medical Systems, Energy Optimization, Sensor Selection, Physiological Behavior Modeling, Behavioral Sensing.

ACM Reference Format:
Noshadi, H., Dabiri, F., Meguerdichian, S., Potkonjak, M., Sarrafzadeh, M. 2011. Behavior Oriented Data Resource Management in Medical Sensing Systems. ACM Trans. Sensor Netw. V, N, Article A (January YYYY), 26 pages.
DOI = 10.1145/0000000.0000000 http://doi.acm.org/10.1145/0000000.0000000

1. INTRODUCTION

Embedded networked systems and wide area cellular wireless systems are becoming ubiquitous in applications ranging from environmental monitoring to urban sensing. Meanwhile, sensor networks have emerged as an important class of distributed embedded systems capable of solving a variety of challenging monitoring and control problems in a number of application domains, ranging from government and military applications to seismic, habitat, and wildlife continuous observations. These technologies have recently been adopted to support the emerging work in medical devices equipped with sensors, known collectively as Wireless Health [Jacobsen et al. 2000] [Jafari et al.

[1]This article is the extended version of the paper titled Energy Optimization in Wireless Medical Systems Using Physiological Behavior, published in Wireless Health 2010. The current version submitted to TOSN has the following materials added to conference version: (1) Collaborative prediction, where more than one predictor is used to predict base sensors. (2) Time-partitioned prediction and its effect on sensors mutual prediction accuracy. (3) Opportunistic sampling. (4) Experiments demonstrating the effect of newly introduced concepts on energy consumption and prediction accuracy. (5) Comprehensive evaluation of the prior work for each described concept in our current work.

2005] [Wu et al. 2008] [Malan et al. 2004]. Wireless Health merges data, knowledge, and wireless communication technologies to provide health care and medical services such as prevention, diagnosis, and rehabilitation outside of the traditional medical enterprise.

Such sensor systems have high potential to significantly improve the quality of life for large segments of the population and enable conceptually new types of applications. However, it is important to note that a path to industrial realization has been more elusive than initially was expected due to a variety of issues, including system and operational complexity, cost and energy sensitivity, semantic complexity, and the need for often revolutionary changes in consumer behavior. Ever-increasing opportunities in health care have thus motivated researchers in Computer Science and Electrical Engineering to develop technologies that can be adopted in the medical and physiological fields and to serve the recently growing demand of low cost and widely accessible health care services.

In this paper, we show how signal processing techniques (time-shifting and segmentation) and adaptive opportunistic sampling, in addition to a new combinatorial optimization paradigm (pseudo-exhaustive combinatorial search), can be used to design an energy optimized embedded sensing system to reduce energy consumption by more than an order of magnitude. While some of these techniques best perform on embedded sensing systems that share local communication, a majority of them can be applied on essentially any sensing system with intrinsic behavioral properties.

Our goal is to demonstrate that often expensive wearable sensing systems used in medical studies can be made more attractive to daily usage through a system of coordinated design and operational techniques that facilitate mass production, customization to specific customers, and low power operation.

Specifically, our optimization goal is to simultaneously minimize the cost (i.e. the number of sensors) and energy consumption (i.e. the weighted sum of collected and communicated samples) while preserving a specified accuracy of collected data, or vice versa. In this paper we focus on wireless communication energy consumption rather than signal sensing energy since sensing energy consumption is negligible compared to that of wireless communication. To do so, we exploit intrinsic space and temporal correlations between sensor data while considering both user and system behavior. Our proposed methodology takes advantage of signal semantics and predictability among sensors to reduce the number of sensors and amount of data acquisition, and has the following technical novelties:

Signal time-shifting: In many sensing systems, relative time shifting greatly improves predictability. This phenomenon is strongly present in medical sensing systems. Another important observation is that cross-correlation functions are almost always unimodular. Therefore, binary search can be used for very fast calculation of the best shifts. In addition, note that the complexity of the sensor selection problem does not increase since we can always shift the selected signals by any required amount.

Signal segmentation for mutual sensor prediction: Signals in many types of embedded sensing systems have natural phases. For example: temperature and humidity are often highly impacted by sun activity, which is composed of morning, afternoon,and night phases; a heart beat has systolic and diastolic phases; and shoe pressure sensors are subject to airborne, landing, and take-off phases. Once the signals are aligned using signal time-shifting, the prediction of signals in each phase is much more accurate after segmentation, because data in one segment will otherwise often act as noise for data in another.

Subset node selection: It is easy to see that the selection of subsets of sensors from which the values of all other sensors can be computed within a given error can be mapped to the dominating set problem, which we solve using a novel type of construc-

tive algorithm that facilitates an easy trade-off between the quality of the solution and the run time. Combinatorial iterative component assembly (CICA) iteratively builds a number of partial solutions that are likely to be part of the final solution. It can be easily shown that an arbitrarily close approximation can be achieved at the expense of run time. Much more importantly, CICA has very strong practical performance.

Opportunistic sampling: The time-shifted nature of signals is also our basis for opportunistic sampling, where a small subset of sensors is regularly sampled while other sensors are placed in sleep mode. Sampling sensors in sleep mode is adaptively controlled by active sensors and data collection starts based on certain event detection by the active sensors. For example, the length of the airborne phase or when a person is standing still may be used for significant reduction in sensor sampling to achieve energy savings.

We present the related work in Section 2. Low power wearable sensing system that has been the main motivation behind this study is presented in Section 3. In Section 4, we present signal properties of this system, which are influenced by user behavior and of which we take advantage for optimization. In 5, we mathematically formulate the relationships between pairs of sensors, derive the predictor-to-base sensor model, and define the predictor selection objectives. Section 6 describes the algorithm for sensor selection. In Section 7 we present the opportunistic sampling and show how prior knowledge of human behavior is used for identifying reliable triggering predictor. Finally, section 8 presents experimental results and our achieved performance. In addition we discussed the changes in prediction error in different types of ambulation and measurement of gait parameters.

2. RELATED WORK

In this section, we briefly overview the most directly related work in low power medical sensing system design, energy optimization in body sensor networks, sensor reading prediction, adaptive opportunistic sampling, and signal segmentation that is related to each step of our work.

Wearable platforms and applications: The convergence of sensing, communication, computation, and storage technologies created the notion, testbeds, theory, and conceptual foundation for sensing networks. Growing interest in designing body sensor networks (BSNs), sensor-based medical devices, and wearable embedded sensor systems attracted an intensive and fast growing research and industrial interest [Jacobsen et al. 2000] [Lo and Yang 2005] [Pantelopoulos and Bourbakis 2010]. A range of wearable platforms have been developed for general signal and physiological parameter collection [Jafari et al. 2005] [Lorincz et al. 2004] [Woo 2006] as well as measuring body movement and activity [DeVaul et al. 2003] [Otto et al. 2006] [Choudhury et al. 2008] [Jafari et al. 2007]. Some platforms have been designed with focus on a fixed set of activities (such as movement classification) [Ganti et al. 2006], while others are more general purpose and are designed for clinical applications that require high fidelity data [Lorincz et al. 2009]. Some wearable systems have been proposed for monitoring the athletic performance in a variety of sports such as skiing, baseball, martial arts, tennis, and golf. These systems are mainly designed for short term use during training sessions. [Michahelles and Schiele 2005] proposed a system to assist and guide professional skiers; [Ahmadi et al. 2006] analyzes the hand's swing during tennis serves; [Ghasemzadeh et al. 2009] measures wrist rotation for golf swings; [Aylward and Paradiso 2007] measures pitches during baseball; and [Kwon and Gross 2005] is used for martial arts training. A number of projects have been focused on application specific medical monitoring. [Wu et al. 2008] uses a smart cane, instrumented with accelerometers and gyro, as an assistive device for geriatric patients. [Erickson et al. 2009] used RFID sensor networks and accelerometers to measure foot

pronation. Another set of projects have used a shoe integrated wireless sensing system for medical monitoring. [Bamberg et al. 2008] embedded pressure sensors inside the shoe and mounted accelerometers and gyro at the back of the shoe to perform gait measurement. A gait phase detection sensor embedded inside the insole is introduced in [Popovic et al. 2004]. [Dabiri et al. 2008] used an instrumented insole inside the shoe as an assistive device for neuropathy. [Oshima et al. 2009] placed accelerometers and pressure sensors inside the shoe to measure walkability. The main differentiator between our work and the above mentioned special purpose systems is that we take the data collected from the sensing environment into consideration while designing the system. Our end design is influenced by users' physiological behavior and takes advantage of its intrinsic properties to produce a power efficient system.

Energy optimization: From the very beginning, it was realized that energy is one the most strict constraints in many classes of sensor networks [Ganesan et al. 2002] [Polastre et al. 2004]. Energy optimization is especially important in the medical domain, where low cost and ease of everyday use is crucial. Thus, it has been targeted by a range of researchers from communication and signal processing to hardware design and software engineering in body area networks. The energy optimization has been addressed on the hardware level, where either hardware responsible for data acquisition and transmission is designed to be energy efficient [Au et al. 2007] or energy scavenging techniques are proposed to make the wearable system power autonomous [Leonov et al. 2005]. Power efficient sensing algorithms and strategies also have been proposed to address the power issue by using smart sensor placement, sensing, and transmission [Ghasemzadeh et al. 2008] [Liu et al. 2007] [Yan et al. 2007] [Xiao et al. 2009]. Surprisingly there are few reports related to cost and energy minimization for medical sensing systems, and to the best of our knowledge, there are no reported techniques for simultaneous minimization of used sensors and the energy budget in wearable systems as our proposed method does.

Signal segmentation: Signal segmentation has been studied in the context of activity recognition and classification. In the segmentation phase, similar to our approach, the goal is to segment sensor readings into basic components. Transcripts of basic motions, called primitives, are proposed in modeling to reduce the complexity of sensing data in motion tracking systems. Most of the previous work has proposed the use of inertial sensors, such as accelerometers or motion capture cameras. [Guimaraes and Pereira 2005] proposed a Human Activity Language, which derived from decomposing angles of body segments calculated from cameras. Unsupervised learning in the recognition system based on motion primitives is proposed by [Husz et al. 2007]. Authors in [Niwase et al. 2005] constructed walking patterns by extracting a sequence of primitives, which is expressed as motion, using Hidden Markov Model. In [Fihl et al. 2006], edit distance is used to distinguish among motion primitives in 3D movement classifier. [Stiefmeier and Roggen 2007] has proposed a string matching technique for real-time gesture spotting. Finally, [Ghasemzadeh et al. 2010] proposed a technique to construct motion transcript from inertial sensors and identify human movement by taking the collaboration between nodes into consideration. In contrast with the above mentioned approaches our goal in this paper is not automatic segmentation / classification of human movement, and we do not use inertial sensors. Our approach takes advantage of prior knowledge of human physiological behavior and uses plantar pressure data for segmentation.

Sensor prediction: Exploration of the correlation of sensor readings is probably the most addressed task in embedded sensing. There are a large number of techniques ranging from a priori assumed dependency (e.g. Gaussian and random Markov fields) and similarity to movie streams [Goel and Imielinski 2001] to non-parametric studies that exploit properties of signals such as monotonicity [Koushanfar et al. 2006].

Opportunistic sampling: Determination of optimal periodic sampling rates and techniques for adaptive sampling have demonstrated their benefits in many embedded sensing environments [Batalin et al. 2004] [Gandhi et al. 2007]. [Malinowski et al. 2007] and [Jevtic et al. 2007] have addressed sampling problems that are related to event-driven sensor sampling activation and therefore to our notion of opportunistic sampling. In addition, recently several distributed event-triggered sampling strategies have been discussed in [Wan and Lemmon 2009]. Also, [Koushanfar et al. 2006] and [Liu et al. 2002] discussed techniques for dynamic sensor node activation.

The main difference between the aforementioned works and ours is that, since sensors in medical shoes directly share electronics and computational resources without the need for mutual wireless communication, we are able to consider much more aggressive sensor sleeping policies and accomplish higher energy savings.

3. PRELIMINARIES

We will demonstrate our proposed methods for an instance of expensive systems used in medical studies for daily and ubiquitous usage. The target system is a lightweight smart shoe capable of sensing plantar pressure, movement, direction, and rotation. This system can be very attractive for a range of applications, such as instability and gait analysis outside of a laboratory environment, outdoor gaming, sports, workplace safety, and environmental data collection. In almost all of those specified applications, long term and continuous operation is required, while in the outdoor environment charging the batteries of the system is not a convenient or even possible task. High sampling rate, continuous data collection, and large-volume data transmission have introduced tremendous challenges to operating such a mobile platform. Considering the aforementioned issues, it is essential to develop a new method for instrumenting the shoe with sensors in a way that would reduce the total system's energy consumption. In Section 3.1, we explore the architecture of the designed lightweight system.

In general mobile or lightweight embedded sensing systems, wireless communication is provably one the most power hungry units in the system. In the system under study in this paper, we have used MicroLEAP as our main sensor node, which is responsible for sensing and transmitting the collected data from the sensors. Table I summarizes the power and energy consumption of the radio and the processor on MicroLEAP [Au et al. 2007].

Table I. MicroLEAP energy consumption

	Power (mW)	Data Rate (kbps)	Energy/Bit (nJ/bit)
Processor	2.7	NA	NA
Radio	57.5	250	230

Therefore, one can easily conclude that in a network of N sensors, eliminating the sampling of a subset of the sensor data can drastically reduce the required energy consumption. Keep in mind that our goal is not to disregard the data from those sensors but provide a means to retrieve the information later on. In other words (as described in detail in Section 5), in this research one of our goals is to sample only a small subset of sensors, and later, in the base station, predict accurately the data values of the whole sensor network.

3.1. System Set Up and Instrumentation

The designed smart shoe is instrumented with pressure sensing material and an embedded data acquisition unit with processing and radio transmission capability. For the pressure sensing material, we either use passive resistive sensors produced by

Fig. 1. Right: medical shoe instrumented with pressure sensors. Left: pressure sensor location map under the foot for Pedar's insole. Sensor placement and location are derived from studying Pedar's insole, which has 99 sensors.

Tekscan [tek] or the piezoresistive fabric produced by Eeonyx [eeo]. When using passive resistive sensors, sensors are placed under the insole and are connected to the data acquisition unit. In the case of the piezoresistive fabric, the fabric will be cut such that it covers the entire surface under the foot, and two conductive layers will be placed on both sides of the fabric. The sensing areas are the parts of the fabric covered by conductive material on both sides. In order to record the pressure values, the sensing area will be connected to the data acquisition board. The processing unit samples data from pressure sensors at 60 Hz. In addition to pressure sensors, the medical shoe also has gyroscopes and accelerometers, which are used for activity recognition, motion tracking, and gaming applications.

Sensor placement, especially for resource-constrained systems, requires sufficient understanding of the environment where the sensors are being deployed so that (1) *decisive and important* areas are covered and (2) resource usage is done intelligently, meaning one does not deploy more resources than necessary. Therefore, we require a deeper understanding of the pressure distribution and behavior beneath the foot so that we can meet all the required objectives and system constraints for sensor placement. These objectives are: energy requirements, sampling accuracy, coverage, etc.

To better understand the signals resulting from the exertion of pressure by both feet, we use a plantar pressure mapping system that covers the entire surface under the foot. The advantage of using such a system is that it gives us a clear picture of the complete pressure distribution under the foot. Pedar [Ped] is an accurate and reliable pressure distribution measuring system for monitoring local loads between the foot and the shoe. It is comprised of insoles equipped with a grid of 99 pressure sensors, which cover the entire area under the foot, and a data acquisition unit capable of data sampling and transmission to a PC over a wireless (bluetooth) connection. Even though systems such as Pedar can provide complete information about the plantar pressure, high data sampling and transmission rates make systems such as Pedar unpopular for low power applications, due to the short lifetime of the system.

4. SIGNAL PROPERTIES

We study plantar pressure signal properties corresponding to human ambulation in order to identify physiological and behavioral trends. The extracted patterns and signal semantics, along with behavioral properties, are used in this study to model the relationship among plantar pressure signals.

A plantar pressure signal can be segmented based on its behavior, which is imposed by human gait characteristics. We divide each step into three segments: (1) airborne; (2) landing; and (3) take-off. Figure 3 demonstrates the extracted segments in the plantar pressure signal. The airborne state is defined as the time during which a particular foot is not touching the ground. The landing state is defined as the time from when the

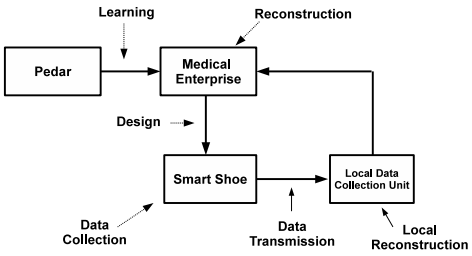

Fig. 2. Overview of the entire system. Once the whole plantar pressure is studied, it is used to design the lightweight / low-power smart shoe. The collected data will be transmitted to the local collection unit, through which it will be sent to the medical enterprise. In both the local collection unit and medical enterprise, collected data will be used to reconstruct all the sensor values.

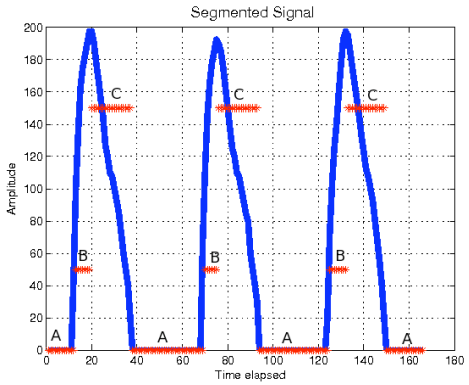

Fig. 3. Three steps with three extracted states each: (A) airborne, (B) take-off and (C) landing.

signal starts increasing its amplitude from the base offset value (calibrated zero pressure) until exactly before it starts decreasing its value; the landing state for each part of the foot, then, is the time during which the body's weight is applied to that particular sensor. Finally, the take-off state is the time interval during which the signal's amplitude decreases from its peak to the base offset value.

Pressure signal characteristics such as morphology, amplitude, and pattern are influenced by an individual's physiology and walking behavior. For example, Figure 5 shows pressure readings from all 99 sensors recorded from Pedar for two test subjects, two steps each, where one had flat feet and the other had hollow feet. As the figure suggests, the active pressure area is greater for the flat-footed person, while the amplitude difference between the active pressure and passive pressure areas for the hollow-footed person is much higher.

The maximum amplitude of a signal is dependent on the relative position of the sensor to the person's center line of pressure progression under the feet; sensors closer to the center line of pressure will record higher pressure values compared to those that are located at the border of the active and passive pressure areas. Sensors that are located on the center line of pressure or on the lines parallel to it demonstrate almost

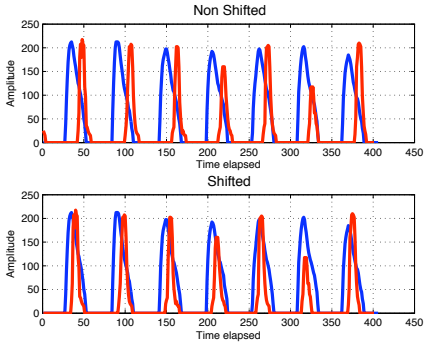

Fig. 4. Top: base and predictor signals at original times. Bottom: base signal time-shifted toward predictor signal, where resulting signals are almost identical.

identical behavior but at different times. Therefore, we can divide the sensors in the active pressure area into sets, where data extracted from all sensors in the same set have similar morphology and almost identical shape when shifted. This implies that the signal's behavior is propagating onto different sensors in the same set. We take advantage of consistent progression in data modeling and predictor selection. Figure 4 shows two signals at their original times and when one is shifted toward the other.

5. PREDICTION MODELING

In order to predict the behavior of the sensors from each other, it is essential to use a good prediction model to minimize prediction errors. Due to sensors' diverse locations and their behavior under the foot during human motion, it is impossible to have a single fitting model to be used as the prediction function across sensor pairs. Therefore, in order to avoid cost and complexity of managing many prediction models, we take advantage of shifting signals. Due to consistent propagation of applied pressure under the active pressure sensing area, there exists a shift for a potential base sensor toward the predictor sensor's direction, which will align the two sensor values such that they will have an overlap between their landing and take-off states. Our measurements show that once the base sensor is shifted toward the predictor sensor such that there is an overlap among their landing and take off states, we will need 3 different mathematical models to present the best prediction function between any two pairs of sensors. The first fitting model is a linear function, while the other two are isotonic. The linear model is the best predictor when two pairs of sensors have complete overlap between landing and take-off states. The other two isotonic models, which are composed of piecewise linear and quadratic models, are the best predictors when take-off and landing states of the base sensor and the predictor sensors are not completely aligned together and either or both are aligned with the other's airborne state.

Figure 6 demonstrates the fitted linear curve and the isotonic curves, which illustrates the mathematical relationship between values from two different pairs of sensors, namely the *predictor* and the *base sensor*.

5.1. Prediction Error

We have considered two objectives for prediction accuracy, while fitting the data using the above specified prediction functions. The first objective was to create the model such that it minimizes the sum of the squares of the residuals or least square as described in Equation (1), which is basically the least-squared method (ls). The second

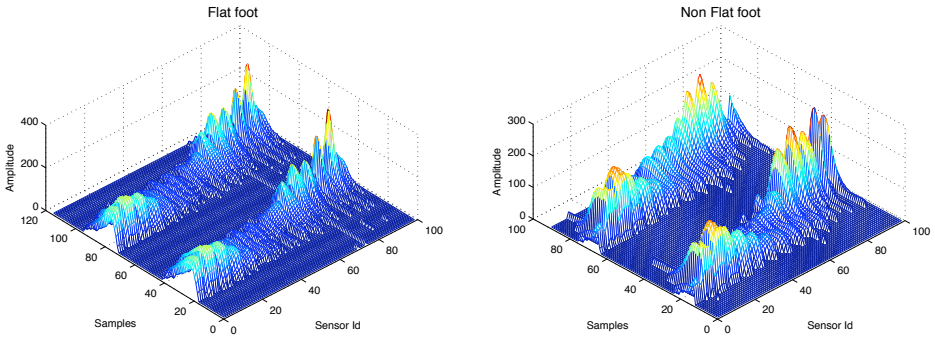

(a) (b)

Fig. 5. Pressure mapping under the feet for (a) flat feet and (b) hollow feet. The progression of pressure sensors over the active pressure area is observable in both cases. The locations of sensors under the foot are based on the pressure sensor map in Figure 1.

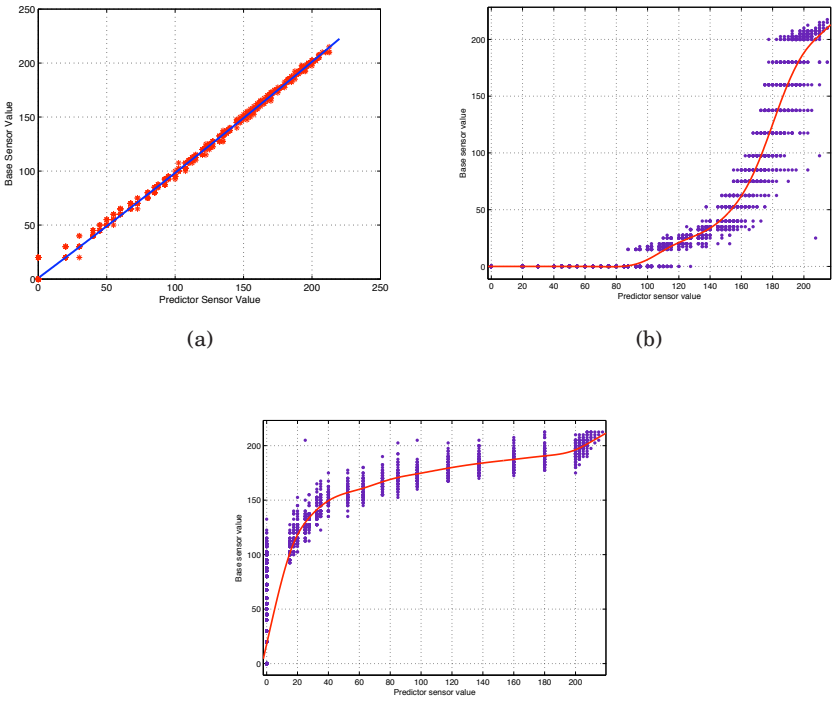

(a) (b)

(c)

Fig. 6. Relationship between predictor vs. base sensor when: (a) the take-off and landing states are overlapping; (b) the landing or take-off state of the base is overlapping with the airborne state of the predictor; and (c) the landing or take off state of the predictor is overlapping with the airborne state of the base.

objective was to minimize the sum of the absolute values of the residuals as described in Equation (2), otherwise known as the L1-model.

$$minimize(sqrt\sum_{t=1}^{m} r(t)^2) \tag{1}$$

$$minimize(\sum_{t=1}^{m} |r(t)|) \tag{2}$$

We evaluate the whole process of sensor predictor selection using both of these error definitions.

5.2. Predictor Selection Objectives

Our proposed methodology in this section is aimed to select a potentially small sub set of deployed sensors along with prediction functions such that by only utilizing that small set of sensors, all sensing data can either be measured directly or predicted with an acceptable error bound. Let us consider two sensors s_i and s_j and assume the corresponding sensor values as functions of time are denoted as $g_i(t)$ and $g_j(t)$. For every pair of sensors we create a collection of predictors $\Phi_{ij} = \{\phi_{ij1}, ..., \phi_{ijm}\}$. ϕ_{ijk} represents a predictor function for sensor s_j that is based on shifted values from sensor s_i by k samples. In other words, if the predicted value for sensor s_j is denoted by $g_j^*(t)$ we have:

$$g_j^*(t) = \phi_{ijk}(g_i(t-k)) \tag{3}$$

For a given predictor there is a prediction error associated with it. We use different cost functions for prediction error as described in Section 5.1. For instance, least square based prediction error can be presented as:

$$\varepsilon(\phi_{ijk}) = \frac{\sum_{t=1}^{T}(g_j(t) - \phi_{ijk}(g_i(t-k)))^2}{g_j(t)^2} \tag{4}$$

For a given sensing system, the prediction transform matrix is defined as below:

$$\Psi_{l\times n} = \begin{pmatrix} \ddots & & \\ & \phi_{ijk} & \\ & & \ddots \end{pmatrix} \tag{5}$$

where $l \leq n$ is the number of predictors denoted by $P = \{p_1, ..., p_l\} \subseteq S$. Now we can formally define the problem. Sensor predictor selection objective can be formulated as:

$$minimize(l = |P|) \tag{6}$$

such that:

$$\forall 1 \leq j \leq n, \exists i, s.t. \Psi_{ij} \neq \varnothing \tag{7}$$

$$\forall \Psi_{ij} \neq \varnothing, \varepsilon(\Psi_{ij}) \leq \delta \tag{8}$$

Constraint (7) guarantees that for any given sensor, there is at least one predictor whereas Constraint (8) enforces that maximum prediction error for any given sensor is less than the target threshold of δ, where δ is an input to the problem defined by the user or is application driven.

5.3. Time-Partitioned Predictors

The previous section illustrates how a sensor can be used as a predictor of values for a secondary sensor. One question that immediately arises is what if multiple sensors in some sort of collaborative fashion would predict the values of a secondary sensor. Collaborative prediction can be in the form of continuous multi sensor predictors or a time-partitioned single predictor or a combination of both.

Continuous multi sensor prediction (CMSP) is when multiple sensors are used to predict the values of a target sensor. In such a setting the prediction function can be represented in general format as:

$$g_j^*(t) = \phi_j(g_i(t - k_i), ..., g_{i_{m-1}}(t - k_{i_{m-1}})) \tag{9}$$

where $g_i(t - k_i)$s are the m sensors used to predict sensor j, each with the corresponding shift of $k_{i_{m-1}}$. *Time-partitioned single predictor (TPSP)*, on the other hand, refers to the setting where at each point of time, one sensor is responsible for prediction and that sensor varies across time based on some conditions that we cover in this section. The time domain is divided into segments τ_is, and within each segment one sensor is responsible for the prediction. To represent TPSP formally, we define a partition selector function $T_p(t, s_j) = s_i$ where t is the sample number or time stamp and s_j is the sensor to be predicted. The return value of this function is s_i, which is the best predictor for s_i for that sample. Therefore TPSP can formally be presented as:

$$g_j^*(t) = \phi_j(g_i(t - k_i)) \iff T_p(t, j) = i \tag{10}$$

5.3.1. TPSP $\subset$ CMSP. It is evident from the definition of CMSP that TPSP is a special case of CMSP. Basically, TPSP can be viewed as CMSP where the prediction function (9) includes the partition selector function within itself. The reason we have separated these two is the difference in analytical approach in finding TPSP since solving CMSP can potentially be very hard [2]

5.3.2. TPSP Modeling and Partitioning. In this paper, the partitioning function T_p is defined based on the state of behavior of the human locomotion stages. Basically, the time for each sensor is divided into segments as defined in Section 4 where each segment corresponds to a semantically well defined stage of locomotion. Therefore, the prediction accuracy/performance of sensor s_i is evaluated individually for any of the time partitions. Let us assume the data from each sensor can be divided into k segments or partitions. The prediction relation across to sensors s_i and s_j is constructed as follows. Each sensor is represented with k sub-sensors s_i^l where $l = 1...k$. This representation holds for both the predictor and the sensor being predicted. Figure 7 illustrates and compares TPSP vs single prediction method. Bottom of the figure shows the representation of the predictor s_i in time-partitioned setting. The edge labeled e_{ij}^{ab} corresponds to the prediction error when segment a of sensor s_i is used to predict the values of segment b in sensor s_j.

5.3.3. Time-Shift Normalization. All the prediction functions (such as (3)) are time preserving in the sense that the sample count and the duration to be predicted is the same as the sample count and duration of the source data. When it comes to TPSP, in order to maintain consistent partitioning of the sensors, segmentation of all sensors should lead to the same-length intervals within each period. In other words, we need

[2]The claim that CMSP is *very hard to solve* is not supported by any analysis and is only based on the observation that even the best selection of a subset of sensors itself can be an NP-Hard problem.

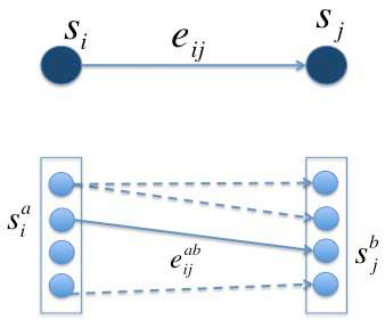

Fig. 7. Predictor time-partitioning; s_i^a represents the sensor i data during stage/segment a; the same notation holds for predicted sensor b.

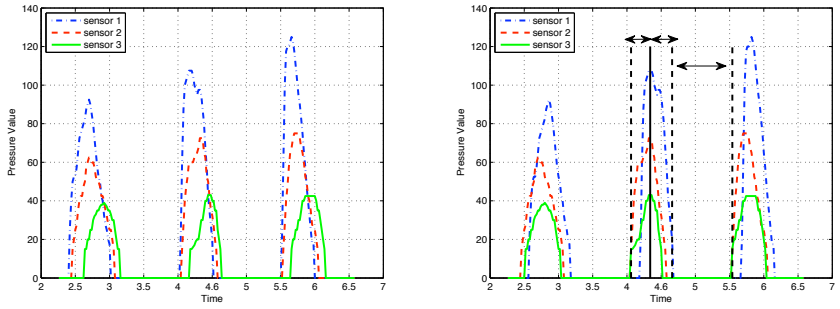

Fig. 8. Raw pressure patterns from three sensors (left) and after time-shift normalization. Unified signal segments are illustrated for the middle period in the bottom plot.

a unified segmentation of the sensor data so that the duration of a particular segment is the same across all the sensors. To better illustrate this notion, we have plotted the data for three sensors in Figure 8.

In this figure, the pressure values from three sensors are normalized in time so that the three predefined pattern segments (as described in Section 4) have the same length in time. Therefore, when it comes to TPSP, we guarantee that dividing the sensors as shown in Figure 8 will lead to mutually disjoint coverage of the predicted sensor and there is a one-to-one mapping from the samples used for prediction to samples to be predicted.

6. PREDICTOR SELECTION

In this section we cover the steps involved in the sensor selection process.

First step of the process is to generate the prediction functions ϕ_{ijk}. Each sensor is potentially a predictor. In the context of prediction, we refer to predictor sensors as p_i and the sensors being predicted are denoted as base sensors, s_i. For a given predictor sensor p_i we generate $n \times m$ predictor functions: $\{\phi_{ijk}\}$ where $1 \leq j \leq n$ and $1 \leq k \leq m$. A prediction error corresponds to each predictor function represented as ε_{ijk} which is computed using Equation 4. Predictor functions are generate as described in Section 5.1.

Top predictor set of sensor s_j is defined as:

$$T_j = \{p_{i_1}, ..., p_{i_k}\} s.t. \varepsilon_{p_i jk} \leq \delta \tag{11}$$

For each sensor which is a top predictor (i.e. $\forall p_i \in \cup T_j$) we create a set of base sensors which that predictor is among the top predictors. In other words:

$$\pi_{p_i} = \{s_{j_1}, ..., s_{j_l}\}, s.t. \forall s_j \in \pi_{p_i}, p_i \in T_{s_i} \tag{12}$$

Basically, π_{p_i} represents the sensors which can be predicted by sensor i with prediction error less that δ.

6.1. Combinatorial Iterative Component Assembly

The goal in sensor selection is to find a minimal set of predictors, $\Pi = \{p_i\}$, which can be used to predict all other sensors. Formally this objective can be stated as minimizing $|\Pi|$ such that:

$$\forall s_j, \exists p_i \in \Pi, s.t. p_i \in T_j \tag{13}$$

We call this minimal set Π^*. The way we tackle this problem is to select a minimum number of π_{p_i}s which cover the whole set of sensors. This problem is equivalent to the minimum set cover problem which is known to be NP-Hard for general graphs. Therefore, we used a combinatorial iterative component assembly algorithm or CICA to find the min set cover. We compare performance of CICA with a well known approximation algorithm described in [Slavík 1996]. In the experimental results we show that CICA is indeed performing better than above mentioned approximation. CICA works in the following way. First it will sort the set of predictors based on maximum number of sensors they can cover. Then it picks top predictors from sorted list and combine each with the initial list and create new set of predictors to base sensors map. The following process continues until there is at least one single set, which covers all the sensors. Algorithm 1 summarizes the process.

ALGORITHM 1: Minimum Set Cover Using Combinatorial Iterative Component Assembly

```
Input: π_{p_i} for all sensors in the system and k for top set selection threshold
Output: Π* minimum set of sensors, which can be used to predict other sensors
Γ ← Sort π_{p_i}s based on number of sensor they can predict in descending order and peak top K sets
ϒ = { }
Index = { }
while no set in Γ covers all sensors in the system do
    for each set γ_i in Γ do
        for each π_{p_i} from Input do
            Combine covered sensors in γ_i and π_{p_i} and add the new set to ϒ
            Add predictor sensor to γ_i's corresponding index.
        end for
    end for
    Γ ← Sort sets in ϒ based in number of sensors they cover in descending order and peak top k sets
end while
Π* ← Index corresponding to largest set in Γ
return Π*
```

Once Π^* is created, we generate the Φ matrix and sensor selection process is completed. We created the elements in Φ matrix in the following way. Rows of the matrix correspond to the predictors in Π^* and the entries of the matrix are

$$\Phi[p_i, j] = argmin(\varepsilon(\Psi_{p_i jk})), if p_i \in T_j \quad (14)$$

$$\Phi[p_i, j] = \varnothing, otherwise \quad (15)$$

In other words, in the column corresponding to base sensor s_i, we insert the best prediction function from its top predictors. Algorithm 2 summarizes the process.

ALGORITHM 2: Minimum Predictor Selection

1: Create prediction functions, ϕ_{ijk}
2: Find top predictors T_{s_i} for every base sensor s_i
3: Using T_js, create the set of base sensors (π_{p_i}) best predictor by every top predictor p_i.
4: Find the minimum set cover from π_{p_i}s and add the corresponding predictors to Π^*
5: Use Π^* to create the prediction matrix Φ

6.2. Generalized Sensor Selection

In general, sensor networks are deployed in a particular environment to collect specific information from that environment. Any optimization of configuration methodology will be applied to that sensor network either prior to deployment or afterward. Many of the environment-dependent offline methodologies need to be repeated if a new sensor network is to be deployed in a new place. For the case study in this paper, the sensing environment is the human body (in particular, the feet). Therefore, for any new test subject, some training data should be collected to efficiently select the best predictors and customize the system accordingly. At the same time, it is only natural to assume that, across different people, the sensing environments have some similarities that might cause repeating predictor selection for any new test subject redundant. To overcome this problem we also tried to find the globally minimum top predictors across all subjects. To achieve this, we simply modified the process as follows. We defined π_{p_i} to be:

$$\pi_{p_i} = \{s_{j_1 O_1}, ..., s_{j_l O_r}\} \quad (16)$$

where O_k represents the kth subject, and r is the total number of subjects under study. Basically, base sensors are differentiated across subjects with the secondary O_k index, but predictors remain the same. Therefore, the number of base sensors to be covered by min set cover is increased by a factor of the number of test subjects. The rest of the process remains the same.

The main question to address is: how stable are the global predictors? In other words, if the top predictors are selected based on training data from k test subjects, how will those predictors perform for the $kth + 1$th test subject? Experimentally we show that once the number of test subjects for global predictors is around 5, the corresponding predictors are in fact global and reliable for any new subject. Figure 9 shows the number of predictors for various numbers of test subjects and error rate bounds. We generated this graph by running, for a given number of test subjects (say k), the generalized predictor selection of all combinations of k test subjects for whom we had reported the average predictor size. It is clear from this graph, the predictor size converges very fast once the number of test subjects passes 7. This means that, once the global predictor

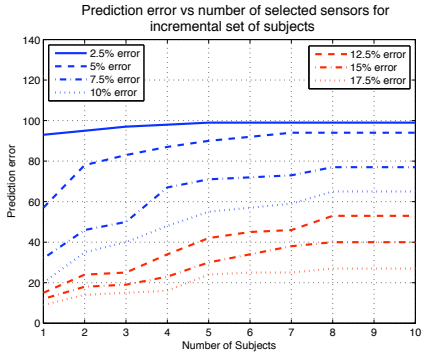

Fig. 9. The number of predictor sensors converges for the generalized case.

set is calculated for a few test subjects, these predictors can be reliably used for a new subject.

7. OPPORTUNISTIC SAMPLING

In many environments monitored by sensor networks, individual sensor data only contain useful information for subintervals of time. In these scenarios, sensors usually record constant values until an *event* is triggered which alters the values recorded by a sensor. For instance, sensor networks deployed for motion detection and object tracking will collect useful data once the presence of a moving object is detected [Klingbeil and Wark 2008]. This does not mean that the sensor values when no moving object is present are not useful; they are constant values and are known beforehand.

In the case of pressure patterns under the foot, the case study in this paper, we see a similar situation. Once the foot is above the ground, all sensor values are zero and data becomes interesting only when the foot touches the ground again. The idea behind opportunistic sampling is to turn off data sampling from a subset of sensors and turn sampling back on when we know some event is occurring. Consider a snapshot of the data from two sensors as shown in Figure 4. As discussed before, the non-trivial information is when the sensors are recording non-zero values. In the context of foot pressure monitoring, we define an *event* to be the duration during which a sensor's value is *not constant*; furthermore, *event triggering time* is the time stamp (or sample) when the event starts, which for sensor s is denoted as t_s^e. This figure suggests that the two sensors shown trigger in the same order in all steps for a similar type of ambulation. In general, there can be many pairs of sensors in the network for which triggering happens in the same order. For example, while walking, a sensor located in the heel side will get triggered before another sensor located on the toe. Let the sensor on the heel be u and the one on the toe be v. Intuitively, if we take the sensor u as the base sensor, sampling of sensor v can start after sensor u is *triggered*. The difference between the times when these two sensors trigger is called the triggering distance, $td = t_u^e - t_v^e$. If $td = K$, then instead of sampling v all the time, we can turn off sampling of v and re-start it K samples after u is triggered. This approach in practice can have two energy-related benefits: 1) reducing sampling energy and 2) reducing transmission energy for sensors like v whose activation can be predicted.

7.1. Reliable Triggering Predictors

Here we define the triggering prediction formally. Sensor u can be a triggering predictor of sensor v iff td_{uv} can be determined with high degrees of certainty. This means that across different time frames, the triggering distance between u and v, td_{uv} should

be easy to calculate so that no information is lost with predictive sampling. There is no doubt that td_{uv} will vary if an object changes its speed of walking or for many other reasons. Assume the period of the current pressure waveform is T. Then, the normalized triggering distance ntd is defined to be $\frac{td}{T}$. We define *triggering prediction reliability*, or TPR, as a measure of how well a sensor can predict the triggering of another sensor:

$$TPR_{uv} = \sigma^2(ntd) \tag{17}$$

which is basically the standard deviation of normalized td_{uv} across a set of periodic activities. This means that, if TPR_{uv} is small, using the current signal period, u can calculate td_{uv} reliably. Now we can define the triggering prediction relation formally:

$$f(u,v) = \kappa, TPR_{uv} \leq \delta \tag{18}$$
$$f(u,v) = null, TPR_{uv} > \delta \tag{19}$$

where $f(u,v)$ is the normalized triggering distance between u and v when TPR is smaller than a given threshold κ and is not defined (i.e. u cannot reliably predict the triggering of v) when TPR is not small enough. The next question to be addressed is how to determine the value of κ. As we saw in previous sections, the value collected by a sensor, u, is represented by $g_u(t)$, where t is the sample number or the time stamp. Now, assume that sensor v is being sampled using triggering prediction of u. On the base station, the regenerated values for v, $g^*_v(t)$, will be:

$$g^*_v(t) = g_v(t); sampling - on \tag{20}$$
$$g^*_v(t) = 0; sampling - off \tag{21}$$

Sampling-on and sampling-off intervals are determined by the triggering prediction of u. The error rate for v's values will be

$$err_v = \frac{\sum (g^*_v(t) - g^*_v(t))^2}{g^*_v(t)^2} \tag{22}$$

This error rate solely depends on how well u could have predicted v, which is a function of ntd_{uv} and its discrepancy across periods. We experimentally calculated this error for different sensor pairs and established a baseline of reliable κ. Figure 10 illustrates the notion of precedence and triggering for two sensors and Figure 11 shows the linear relationship of triggering distance to step time. This picture enables us to use the linerly normalize the triggering distance when the step time varies.

7.2. Triggering Predictor Selection Objective

The triggering prediction method can allow for better utilization of resources if the idle period of sensor v compared to the active period is large enough. In other words, if v is mostly active, there is no benefit to dynamically turning sampling on and off. We define a measure of the active length of a sensor as α_s, which is, for a given period T, equal to the ratio of the active interval to T.

Now we can present this method formally. The objective of predictive sampling is to select a subset of sensors (called trigger predictors or TP) which will be monitored all the time and can be used to determine when to start sampling other sensors; this set can yield a minimum sampling across all sensors. Thus, if the sensor set is denoted as $S = s_1, ...s_n$, a feasible set of trigger predictors can be defined as:

$$TP_S \subset S, st. \forall s \in S, \exists q \in TP_S : f(q,s) = \kappa \neq null \tag{23}$$

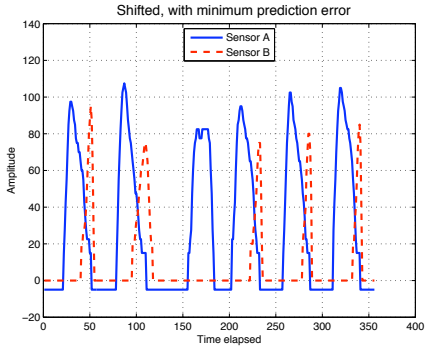

Fig. 10. The relationship between two signals determines the order of sampling in adaptive sampling.

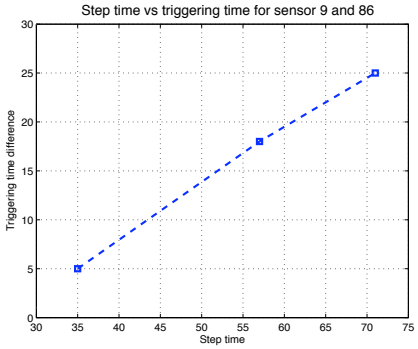

Fig. 11. Relationship between step time and the median time difference between the triggering times of sensor 9, located on the heel, and sensor 86, located on the toe.

The objective becomes to find TP_S^* such that:

$$\sum_{s \in TP_S^*} |g_s(t)| + \sum_{s \in S - TP_S^*} |g_s(t)| \times \alpha_s \tag{24}$$

is minimized, where:

$$\sum_{s \in S - TP_S^*} |g_s(t)| = \sum_{s \in S - TP_S^*} \alpha_s \times I \tag{25}$$

I is the time interval under study.

7.3. TP^* Selection Algorithm

Every sensor can potentially have multiple trigger predictors and itself can predict the triggering of other sensors. In order to find the minimum number of predictors to minimize sampling (and therefore transmission) energy, we construct a triggering graph $G_T = (V, E)$ as follows. Each node in this graph represents a sensor in the sytem, $V = \{s_1 ... s_N\}$. If sensor s_i can be used as a triggering predictor of s_j, i.e. $f(s_i, s_j) = \kappa$ (Equation 18), there will be a direct edge e_{ij} in E. In other words $E = \{e_{ij} | f(s_i, s_j) = \kappa > 0\}$. Note that since triggering relations is determined per period and the triggering

point is the start of the active segment of the pressure pattern, G_T is a directed acyclic graph.

We tackle the problem of finding the best TP using a similar technique to the one described in Section 6.1. In other words, this problem is by nature similar to the *weighted* predictor selection covered in Section 6 with a different definition of predictor sets and the cost function for each set. The predictor sets are defined in Equation 11.

$$\pi_{p_i} = \{s_{j_1}, ..., s_{j_l}\}, s.t. \forall s_j \in \pi_{p_i}, f(p_i, s_j) \neq null \tag{26}$$

$f(p_i, s_j) \neq null$ basically indicates that p_i can reliably predict the triggering of sensor s_j. We run the same CICA algorithm to find the minimal set of triggering predictors, or TP^*.

Furthermore, only minimizing the number of predictors does not optimize the objective. The active segments of sensors have different length, therefore, it is ideal to select triggering predictors that have larger active range or in other words, sample other non-predictor sensors that have the shortest length. Figure 12 illustrates a simple example. Assume that $\alpha_v > \alpha_w$, therefore, the prediction selection in (a) will lead to a better saving by the amount of $(\alpha_v - \alpha_w) \times I$ per interval I.

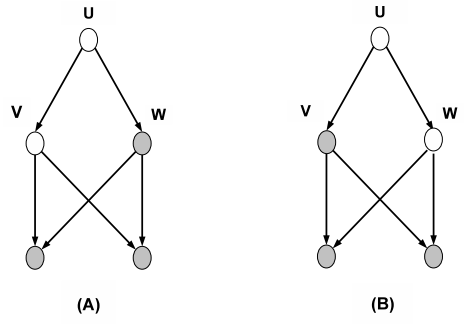

Fig. 12. Triggering graph for a set of 5 sensors and two possible selection scenarios.

In CICA, the comparison across sets is based on the size of the set. Here, we assign a weight to each π_{p_i}

$$w(\pi_{p_i}) = \frac{\sum_{s_j \in \pi_{p_i}} \alpha_{s_j}}{|\pi_{p_i}|} \tag{27}$$

We modify CICA algorithm such that the sorting of sets is done based on the weight function above. Weighted CICA is described in Algorithm 3.

8. EXPERIMENTAL RESULTS

In order to illustrate the effectiveness of the proposed methodologies, we used Pedar to collect sensor data across 10 individual subjects. We tried to keep the subject set as diverse as possible in terms of walking behavior and sensor data variability. The subject set was composed of 7 men and 3 women, where one man and one woman were flat-footed and 2 men were overweight. Foot sizes ranged from 7 to 11.

For the collected data set, we performed minimum predictor selection with three different configurations: 1) least-square method for predictor function generation without any shift in base-sensor data (ls-noShift); 2) least-square method for predictor function

ALGORITHM 3: Weighted Minimum Set Cover Using Combinatorial Iterative Component Assembly

Input: π_{p_i} for all sensors in the system and k for top set selection threshold and α_s for all the sensors.
Output: Π^* minimum set of sensors, which can be used to predict triggering of other sensors
$\Gamma \leftarrow$ Sort π_{p_i}s based on $w(\pi_{p_i})$ in ascending order and peak top K sets (lowest weights)
Υ = { }
Index = { }
while no set in Γ covers all sensors in the system **do**
  for each set γ_i in Γ **do**
    for each π_{p_i} from Input **do**
      Combine covered sensors in γ_i and π_{p_i} and add the new set to Υ
      Add predictor sensor to γ_i's corresponding index.
    end for
  end for
  Recalculate $w(\gamma_i)$ in Υ
  $\Gamma \leftarrow$ Sort sets in Υ based on $w(\pi_{p_i})$ in ascending order and peak top k sets
end while
$\Pi^* \leftarrow$ Index corresponding to largest set in Γ
return Π^*

Table II. Minimum selected sensors using CICA vs Greedy algorithm

Individual			General		
Error	CICA	Greedy	Error	CICA	Greedy
2.5	63	78	2.5	94	94
5	41	52	5	65	82
7.5	21	27	7.5	59	75
10	14	18	10	42	58
12.5	11	15	12.5	42	56
15	5	6	15	24	32
17.5	4	4	17.5	21	27

generation with shift in base sensor value (ls-wShift); 3) segmentation-based predictor function generation using least-square method (ls-segmentation); and 4) L1-method for predictor function generation (L1).

Furthermore, we repeated the above scenarios for the global case where the process was implemented on the aggregated data from all individuals (as described in Section 6.2). 30% of each test subject's data was used to find the best predictor, and the remaining 70% was used to evaluate the accuracy of the prediction functions. We ran the sensor selection process for a range of maximum prediction errors (δ in Equation 8). The maximum prediction error rate ranges from 2.5% to 20%. Afterwards, we simulated the estimated total energy savings on the sensor node (MicroLEAP) when the minimal predictors were used to sample the data. As seen in the system architecture, one sensor node is responsible for sampling and transmission of the data from sensors.

Table II summarizes the performance of the proposed combinatorial iterative component assembly algorithm to find the minimum set cover versus the greedy approach. As table suggests, our proposed algorithm (CICA) outperforms the well known greedy algorithm in both the individual and general case. In the individual case, CICA outperforms the greedy algorithm by an average of 22.3% for error rates between 2.5% and 12.5%, while for 15% and 17.5% errors, the outcome is almost the same for both algorithms. In the general case, CICA outperforms the greedy algorithm by an average of 23.8% for error rates greater then 5%, while for 2.5% the outcome of both algorithms are the same.

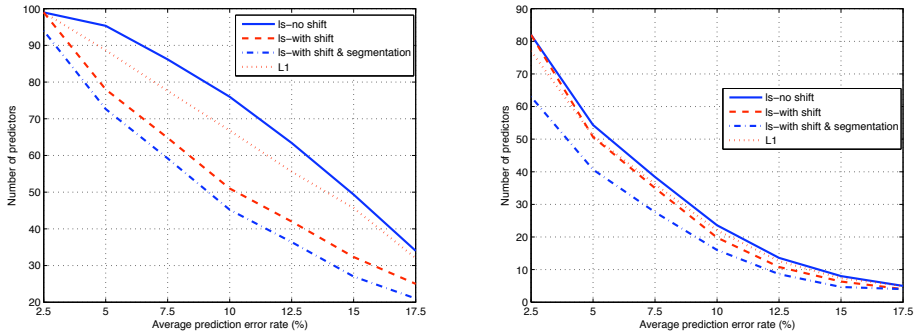

(a) (b)

Fig. 13. Number of predictor sensors vs. the average prediction error for the whole sensing network for (a) the general case and (b) averaged over individual test subjects.

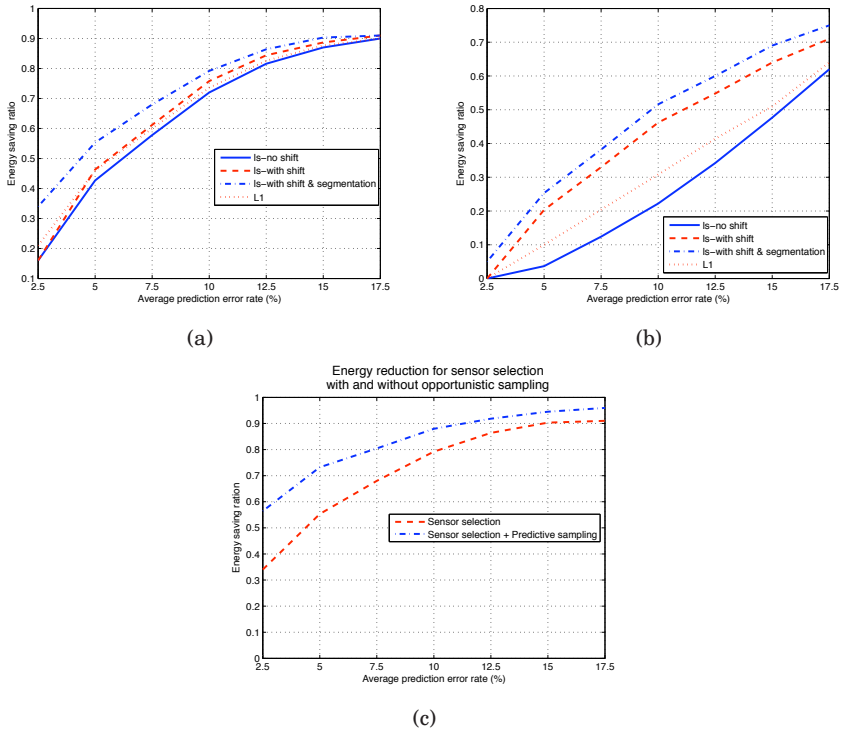

(a) (b)

(c)

Fig. 14. Ratio of energy savings with respect to no prediction vs. the average prediction error for the whole sensing network, for (a) the individual case and (b) the general case. (c) shows the same relation for opportunistic sampling before and after sensor selection.

Figure 13(b) illustrates the number of sensors required to predict the whole sensor network data (out of 99 sensors total) versus the maximum prediction error for the four different scenarios described above. These graphs are averaged over the 10 test subjects we had. Figure 14(a) summarizes the average power savings ratio for different maximum prediction errors. These graphs illustrate that power saving ranges from

18% to 91%, depending on the approach taken, while the maximum prediction error rate ranges from 2.5% to 20%.

Finally, we repeated the same set of experiments and simulations for the general case. Figures 13(a) and 14(b) summarize the results. As expected, the general case tries to find a *global* predictor whose size is usually larger than the predictor set of an individual, and therefore energy saving ranges from 0% to 76%. Note that for a maximum prediction error rate of 2.5%, we must practically select all the sensors, resulting in no energy savings.

8.1. Time-Partitioned Prediction

The previous sections illustrated the effectiveness of various predictor selection and as expected ls-with shift and segmentation led to best sensor reduction and therefore energy savings. Furthermore, we applied time partitioned single prediction (TPSP) as described in Section 5.3.2. In order to keep the graphs readable, we excluded the results of TPSP from Figure 13(b). Figure 15, on the other hand, compares the number of predictor sensors for TPSP vs the best predictor selection in Figure 13(b) which ls-with segmentation and shift. For low error rate thresholds, TPSP can further reduce the number of predictors by 5% to 10% but as the error rate threshold is loosened, or in other words increased, these two approaches lead to very close predictor counts. The main cause supporting this convergence is the fact that for high error rate thresholds, there are few sensors that can collectively predict the network.

8.2. Opportunistic Sampling Data Reduction

We evaluated the effect of opportunistic sampling in two different setups. First, for each individual subject in our experiments, we measured the energy reduction resulting from opportunistic sampling. The way we calculated the energy reduction is similar to the previous section: we calculated the data volume reduction caused by sampling cuts and incorporated that into the energy consumption of the system. Figure 16 illustrates the energy savings across different test subjects. Note that opportunistic sampling by itself can reduce energy consumption from 48% to 66% depending on the individual and his/her motion patterns.

Next, we applied opportunistic sampling on top of predictor selection. First, we found the best predictors with the minimum least square error bounded by a range of values for each individual test subject. Then, for each subject, we applied opportunistic sampling on the predictor set (since that set is the only active set of sensors) and calculated the data transmission rate reduction for the hybrid of these two methods. From there, we estimated the average energy reduction for each bound on error rate. Figure 14(c) shows that opportunistic sampling can further reduce energy consumption from 4% to 21%, resulting in total energy reduction of 56% to 96% depending on the upper bound on error rate.

8.3. Prediction Among Different Types of Ambulation

We computed the prediction error in different human ambulations such as regular walking, slow walking, running, jumping, standing, and walking backward. We preform the experiments based on three sets of selected predictors, for maximum prediction error of 4%, 8% and 12%. We illustrated that selected predictor sensors are good predictors across different types of human ambulation, Figure 17 shows the average prediction error across different ambulation patterns, averaged over test subjects. As the figure suggests, the prediction error only gets higher up to 2% across different ambulations.

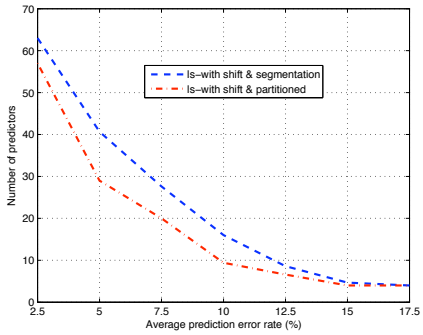

Fig. 15. Comparison of minimum predictors with using time-partitioned multi-predictors.

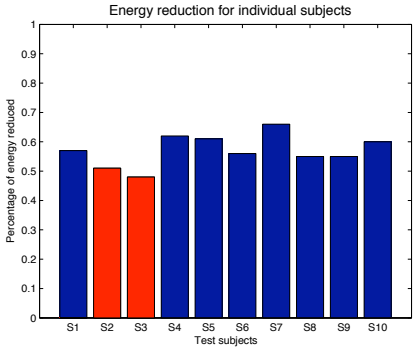

Fig. 16. Ratio of energy savings only using opportunistic sampling. S2 and S3 are flat-footed subjects.

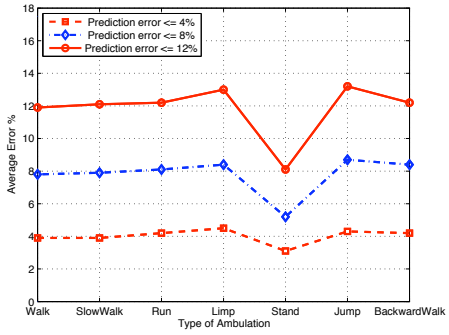

Fig. 17. Comparison of prediction error among different types of human activity and ambulation. As the figure suggests, the reconstruction error is very close in different types of ambulation.

8.4. Computing Gait Parameters and Abnormality

Health monitoring systems are designed to capture and monitor specific parameters and irregular and abnormal behavior. In the context of human locomotion and gait analysis, these parameters of interest are gait features such as stance, swing, stride, step time, etc. [Whittle 2007], which researchers and clinicians are interested to monitor. Furthermore, abnormalities in the same context are defined over these gait param-

eter changes and deviations [Hausdorff et al. 2001] [Hausdorff et al. 1996] [Hausdorff et al. 1999] [Hausdorff 2007] [Maki 1997] [Yenets et al. 2007]. For a design based on our proposal it is important to show that using selected sensors' set it is still possible to measuring the specified features. We demonstrated that that using selected predictor set we can still compute gait parameters accurately. To demonstrate this we first take all sensors into consideration and for each user during different ambulations we computed the gait parameters. Then we take the selected sensors set based on our algorithm for 3 bounded errors (4% to 8% 12%) and reconstruct the values of the rest of the base sensors and then compute the gait parameters.

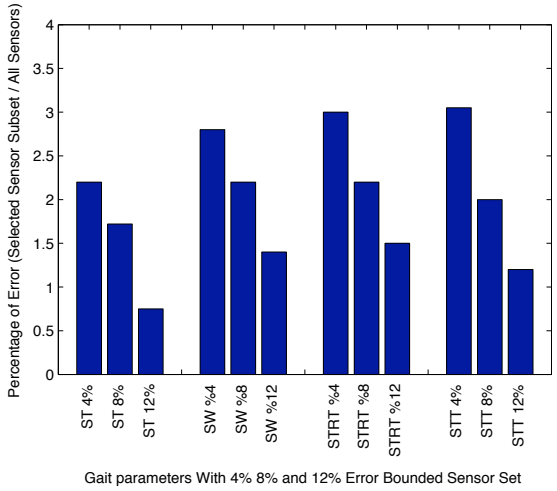

Fig. 18. Percentage of error introduced from calculating gait parameters using selected sensor set with bounded prediction maximum error of 4% , 8% and 12%, with respect to computed gait parameters using all sensors while performing the following types of ambulation: slow walk, run, limp, and backward walk.

Figure 18 illustrates the fact that gait feature measurement error using predictor sensors is very small compared against extracting the same features using all the pressure sensors. This in fact is not surprising since a majority of the gait features capture events which are less sensitive to deviation of a single pressure point. Therefore, as long as we have a bounded prediction error rate for the predictor sensors, we can utilize this small set of sensors to accurately capture gait abnormalities since abnormalities are functions of gait features rather than individual sensor values.

9. CONCLUSION

In this paper, we explored the data volume management and its corresponding implications on energy consumption and system lifetime in embedded and wearable sensing systems through the introduction of multiple stages of signal analysis and optimization algorithms. The high level contribution of this paper is to study signal patterns and utilize them to develop novel *prediction* algorithms at different levels of information flow in such systems. These methods aim to make expensive wearable sensing systems more feasible for everyday use by minimizing sampling sources while enabling reconstruction of the data from all sensors. One goal was to use a subset of sensors to accurately generate the data from all sensors. In other words, the design flow, adapts to the context of the sensing environment and leads to a efficient data management configuration. This goal was achieved by introducing two novel methods for signal shift-

ing, which enables better prediction of sensor data, followed by data segmentation to further enable piecewise predictions. On top of this prediction strategies, the notion of opportunistic sampling was introduced in which even smaller subset of sensors are selected that can predict when to sample the rest of target sensors. To solve the above problems, we also developed an efficient approximation algorithm called combinatorial iterative component assembly (CICA) to select best predictors for each scenario. In order to show the effectiveness of the proposed methodologies, we applied the presented methods on an embedded wearable sensing system equipped with 100 pressure sensors. Experimental results show that the proposed techniques can yield from 56% to 96% in energy reduction while maximum sampling error rate ranges from only 5% to 17.5%.

REFERENCES

Eeonyx resistive fabric. http://www.eeonyx.com.

Pedar: plantar pressure system. http://www.novel.de.

Tekscan pressure sensor. http://www.tekscan.com.

2006. Alarm-net: Wireless sensor networks for assisted-living and residential monitoring. Technical Report CS-2006-11, University of Virginia.

AHMADI, A., ROWLANDS, D., AND JAMES, D. 2006. Investigating the translational and rotational motion of the swing using accelerometers for athlete skill assessment. In *5th IEEE Conference on Sensors*. 980983.

AU, L. K., WU, H. W., BATALIN, M. A., MCLNTIRE, D., AND KAISER, W. J. 2007. Microleap: Energy-aware wireless sensor platform for biomedical sensing applications. In *IEEE Biomedical Circuits and Systems Conference, BIOCAS'07*. IEEE, Montreal, Que., 158–162.

AYLWARD, R. AND PARADISO, J. A. 2007. wearable sensor network for biomotion capture and interactive media. In *The International Conference on Information Processing in Sensor Networks*.

BAMBERG, S., BENBASAT, A. Y., SCARBOROUGH, D. M., KREBS, D. E., AND PARADISO, J. A. 2008. Gait analysis using a shoe-integrated wireless sensor system. *IEEE Transactions on Information Technology in Biomedicine 12,* 4, 413–423.

BATALIN, M. A., RAHIMI, M., YU, Y., LIU, D., KANSAL, A., SUKHATME, G. S., KAISER, W. J., HANSEN, M., POTTIE, G. J., SRIVASTAVA, M., AND ESTRIN, D. 2004. Call and response: experiments in sampling the environment. In *SenSys '04: Proceedings of the 2nd international conference on Embedded networked sensor systems*. ACM, New York, NY, USA, 25–38.

CHOUDHURY, T., BORRIELLO, G., CONSOLVO, S., HAEHNEL, D., HARRISON, B., HEMINGWAY, B., HIGHTOWER, J., KLASNJA, P., KOSCHER, K., LAMARCA, A., LANDAY, J. A., LEGRAND, L., LESTER, J., RAHIMI, A., REA, A., , AND WYATT, D. 2008. The mobile sensing platform: An embedded system for capturing and recognizing activities. *IEEE Pervasive Magazine*.

DABIRI, F., VAHDATPOUR, A., NOSHADI, H., HAGOPIAN, H., AND SARRAFZADEH, M. 2008. Ubiquitous personal assistive system for neuropathy. In *Proceedings of the 2nd International Workshop on Systems and Networking Support for Health Care and Assisted Living Environments*. HealthNet '08. 17:1–17:6.

DEVAUL, R., SUNG, M., GIPS, J., AND PENTLAND, A. 2003. Mithril 2003: applications and architecture. In *EEE International Symposium of Wearable Computing*.

ERICKSON, V., KAMTHE, A. U., AND CERPA, A. E. 2009. Measuring foot pronation using rfid sensor networks. In *SenSys '09: Proceedings of the 7th ACM Conference on Embedded Networked Sensor Systems*. ACM, New York, NY, USA, 325–326.

FIHL, P., HOLTE, M. B., MOESLUND, T., AND RENG, L. 2006. Action recognition using motion primitives and probabilistic edit distance. In *Lecture Notes in Computer Science*. Vol. 37. 375.

GANDHI, S., SURI, S., AND WELZL, E. 2007. Catching elephants with mice: sparse sampling for monitoring sensor networks. In *SenSys '07: Proceedings of the 5th international conference on Embedded networked sensor systems*. ACM, New York, NY, USA, 261–274.

GANESAN, D., KRISHNAMACHARI, B., WOO, A., CULLER, D., ESTRIN, D., AND WICKER, S. 2002. Complex behavior at scale: an experimental study of low-power wireless sensor networks. Tech. Rep. TR 02-0013, UCLA.

GANTI, R., JAYACHANDRAN, P., ABDELZAHER, T., AND STANKOVIC, J. 2006. Satire: A software architecture for smart attire. In *ACM Mobisys*.

GHASEMZADEH, H., GUENTERBERG, E., GILANI, K., AND JAFARI, R. 2008. Action coverage formulation for power optimization in body sensor networks. In *ASP-DAC '08: Proceedings of the 2008 Asia and South Pacific Design Automation Conference*. IEEE Computer Society Press, Los Alamitos, CA, USA, 446–451.

GHASEMZADEH, H., LOSEU, V., GUENTERBERG, E., AND JAFARI, R. 2009. Sport training using body sensor networks: a statistical approach to measure wrist rotation for golf swing. In *Proceedings of the Fourth International Conference on Body Area Networks*. 2:1–2:8.

GHASEMZADEH, H., LOSEU, V., AND JAFARI, R. 2010. Collaborative signal processing for action recognition in body sensor networks: a distributed classification algorithm using motion transcripts. In *Proceedings of the 9th ACM/IEEE International Conference on Information Processing in Sensor Networks*. 244–255.

GOEL, S. AND IMIELINSKI, T. 2001. Prediction-based monitoring in sensor networks: taking lessons from mpeg. *SIGCOMM Comput. Commun. Rev. 31,* 5, 82–98.

GUIMARAES, G. AND PEREIRA, L. 2005. Inferring defince-clause grammars to express multivariate time series. In *Procesings of the 18th international conference on innovation in applied artificial intelligence*. 234–231.

HAUSDORFF, J. M. 2007. Gait dynamics, fractals and falls: Finding meaning in the stride-to-stride fluctuations of human walking. *Human Movement Scienc 26*, 555 –589.

HAUSDORFF, J. M., PURDON, P. L., PENG, C. K., LADIN, Z., WEI, J. Y., AND GOLDBERGER, A. 1996. Fractal dynamics of human gait: stability of long-range correlations in stride interval fluctuations. *Applied Physiology 80*, 1446–1453.

HAUSDORFF, J. M., RIOS, D. A., AND EDELBERG, H. 2001. Gait variability and fall risk in community-living older adults: A 1-year prospective study. *Archives of Physical Medicine and Rehabilitation 82*, 1050–1056.

HAUSDORFF, J. M., ZEMANY, L., PENG, C. K., AND GOLDBERGER, A. L. 1999. Maturation of gait dynamics: stride-to-stride variability and its temporal organization in children. *Applied Physiology 86*, 1040–1047.

HUSZ, Z., WALLACE, A., AND P., G. 2007. Human activity recognition with action primitives. In *Advanced Video and Signal Based Surveillance*. 330–335.

JACOBSEN, S. C., PETELENZ, T. J., AND PETERSON, S. C. 2000. Wireless health monitoring system. US Patent 6,160,478.

JAFARI, R., BAJCSY, R., GLASER, R. S., GNADE, B., SGROI, M., AND SASTRY, S. 2007. Platform design for health-care monitoring applications. In *Joint Workshop on High Confidence Medical Devices, Software, and Systems (HCMDSS) and Medical Device Plug-and-Play (MD PnP) Interoperability*.

JAFARI, R., DABIRI, F., AND SARRAFZADEH, M. 2005. Customed: A power optimized customizable and mobile medical monitoring and analysis system. In *ACM HCI Challenges in Health Assessment*.

JEVTIC, S., KOTOWSKY, M., DICK, R. P., DINDA, P. A., AND DOWDING, C. 2007. Lucid dreaming: reliable analog event detection for energy-constrained applications. In *IPSN '07: Proceedings of the 6th international conference on Information processing in sensor networks*. ACM, New York, NY, USA, 350–359.

KLINGBEIL, L. AND WARK, T. 2008. A wireless sensor network for real-time indoor localisation and motion monitoring. In *IPSN '08: Proceedings of the 7th international conference on Information processing in sensor networks*. IEEE Computer Society, Washington, DC, USA, 39–50.

KOUSHANFAR, F., TAFT, N., AND POTKONJAK, M. 2006. Sleeping coordination for comprehensive sensing using isotonic regression and domatic partitions. In *INFOCOM*. Vol. 1-13. IEEE, Barcelona, Spain.

KWON, D. Y. AND GROSS, M. 2005. Combining body sensors and visual sensors for motion training. In *Proceedings of the 2005 ACM SIGCHI International Conference on Advances in computer entertainment technology*. 94 – 101.

LEONOV, V., FIORINI, P., SEDKY, S., TORFS, T., AND VAN HOOF, C. 2005. Thermoelectric mems generators as a power supply for a body area network. In *TRANSDUCERS '05, The 13th International Conference on Solid-State Sensors, Actuators and Microsystems*. Vol. 1. 291–294.

LIU, J., CHEUNG, P., ZHAO, F., AND GUIBAS, L. 2002. A dual-space approach to tracking and sensor management in wireless sensor networks. In *WSNA '02: Proceedings of the 1st ACM international workshop on Wireless sensor networks and applications*. ACM, New York, NY, USA, 131–139.

LIU, Y., VEERAVALLI, B., AND VISWANATHAN, S. 2007. Critical-path based low-energy scheduling algorithms for body area network systems. In *RTCSA '07: Proceedings of the 13th IEEE International Conference on Embedded and Real-Time Computing Systems and Applications*. IEEE Computer Society, Washington, DC, USA, 301–308.

LO, B. AND YANG, G. Z. 2005. Architecture for body sensor networks. In *Perspective in Pervasive Computing*. 23–28.

LORINCZ, K., CHEN, B., CHALLEN, G. W., CHOWDHURY, A. R., PATEL, S., B.P., S., AND WELSH, M. 2009. Mercury: a wearable sensor network platform for high-fidelity motion analysis. In *Proceedings of the 7th ACM Conference on Embedded Networked Sensor Systems. SenSys '09*. 183–196.

LORINCZ, K., MALAN, D. J., FULFORD-JONES, R. F., NAWOJ, A., CLAVEL, A., SHNAYDER, V., MAINLAND, G., WELSH, M., AND MOULTON, S. 2004. Sensor networks for emergency response: Challenges and opportunities. *IEEE Pervasive Computing 3*, 16–23.

MAKI, B. 1997. Gait changes in older adults: predictors of falls or indicators of fear. *American Geriatric Society 45*, 313 –333.

MALAN, D., FULFORD-JONES, T., WELSH, M., AND MOULTON, S. 2004. Codeblue: An ad hoc sensor network infrastructure for emergency medical care. In *International Workshop on Wearable and Implantable Body Sensor Networks*.

MALINOWSKI, M., MOSKWA, M., FELDMEIER, M., LAIBOWITZ, M., AND PARADISO, J. A. 2007. Cargonet: a low-cost micropower sensor node exploiting quasi-passive wakeup for adaptive asychronous monitoring of exceptional events. In *SenSys '07: Proceedings of the 5th international conference on Embedded networked sensor systems*. ACM, New York, NY, USA, 145–159.

MICHAHELLES, F. AND SCHIELE, B. 2005. Sensing and monitoring professional skiers. In *IEEE Conference on Pervasive Computing*.

NIWASE, N., YAMAGISHI, J., AND KOBAYASHI, T. 2005. Human walking motion synthesis with desired pace and stride length based on hsmm. *IEICE - Trans. Inf. Syst. E88-D*, 2492–2499.

OSHIMA, K., ISHIDA, Y., KONOMI, S., THEPVILOJANAPONG, N., AND TOBE, Y. 2009. A human probe for measuring walkability. In *SenSys '09: Proceedings of the 7th ACM Conference on Embedded Networked Sensor Systems*. ACM, New York, NY, USA, 353–354.

OTTO, C. A., JOVANOV, E., AND MILENKOVIC, A. 2006. A wban-based system for health monitoring at home. In *3rd IEEE EMBS International Summer School and Symposium on Medical Devices and Biosensors*.

PANTELOPOULOS, A. AND BOURBAKIS, N. 2010. A survey on wearable sensor-based systems for health monitoring and prognosis. *Trans. Sys. Man Cyber Part C 40*, 1–12.

POLASTRE, J., HILL, J. L., AND CULLER, D. E. 2004. Versatile low power media access for wireless sensor networks. In *SenSys*. 95–107.

POPOVIC, S., DIETZ, M. R., MORARI, V., PAPPAS, M., KELLER, I., AND MANGOLD, T. 2004. A reliable gyroscope-based gait-phase detection sensor embedded in a shoeinsole. *IEEE Sensors Journal 4,* 2, 268 – 274.

SLAVÍK, P. 1996. A tight analysis of the greedy algorithm for set cover. In *STOC '96: Proceedings of the twenty-eighth annual ACM symposium on Theory of computing*. ACM, New York, NY, USA, 435–441.

STIEFMEIER, T. AND ROGGEN, D. 2007. Gestures are strings: Efficient online gesture spotting and classification using string matching. In *Proceedings of 2nd International Conference on Body Area Networks (BodyNets)*.

WAN, P. AND LEMMON, M. D. 2009. Event-triggered distributed optimization in sensor networks. In *IPSN '09: Proceedings of the 2009 International Conference on Information Processing in Sensor Networks*. IEEE Computer Society, Washington, DC, USA, 49–60.

WHITTLE, M. W. 2007. *Gait Analysis: An Introduction*. Elsevier.

WU, W., AU, L., JORDAN, B., STATHOPOULOS, T., BATALIN, M., KAISER, W., VAHDATPOUR, A., SARRAFZADEH, M., FANG, M., AND CHODOSH, J. 2008. The smartcane system: an assistive device for geriatrics. In *BodyNets '08: Proceedings of the ICST 3rd international conference on Body Area Networks*. ICST, ICST (Institute for Computer Sciences, Social-Informatics and Telecommunications Engineering), Tempe, Arizona, 1–4.

WU, W. H., BUI, A. T., BATALIN, M. A., AU, L. K., BINNEY, J. D., AND KAISER, W. J. 2008. Medic: Medical embedded device for individualized care. *Artificial Intelligence in Medicine 42,* 2, 137–152.

XIAO, S., DHAMDHERE, A., SIVARAMAN, V., AND BURDETT, A. 2009. Transmission power control in body area sensor networks for healthcare monitoring. *IEEE Journal on Selected Areas in Communications 27,* 1, 37 – 48.

YAN, L., ZHONG, L., AND JHA, N. K. 2007. Energy comparison and optimization of wireless body-area network technologies. In *BodyNets '07: Proceedings of the ICST 2nd international conference on Body area networks*. ICST (Institute for Computer Sciences, Social-Informatics and Telecommunications Engineering), ICST, Brussels, Belgium, Belgium, 1–8.

YENETS, J., ELROD, M., AND PERELL, K. 2007. Predicting fall risk with plantar pressure equipment in individuals with diabetes. *Clinical Kiniesology 61*.